The Effect of Interface Modification between POM and PTFE on the Properties of POM/PTFE Composites

CHI-YUAN HUANG, CHAO-I TSENG

Department of Materials Engineering, Tatung University, 40 Chungshan North Road, 3rd Sec., Taipei 10451, Taiwan, Republic of China

Received 16 November 1999; accepted 9 February 2000

ABSTRACT: A plasma technique was applied to modify the surface of polytetrafluoroethylene (PTFE) fiber to improve the compatibility between PTFE and polyacetal (POM). This technique used argon (Ar) plasma to treat PTFE fiber first and then grafting the fiber with acrylic acid (AAc) by peroxidation. The Ar plasma-treated PTFE (PPTFE) fiber and AAc-grafted PPTFE (AAc-*g*-PPTFE) fiber were added into POM to increase the wear resistance and to decrease the friction coefficient of POM. The variables of the experiments were plasma treatment time, monomer concentration of AAc, and grafting time. The graft copolymer was characterized by Fourier transform infrared (FTIR) spectroscopy. The stress–strain behavior, impact strength, Taber wear factor, friction coefficient, and morphology of composites were also investigated. The properties of POM/PTFE composites could be successful modified by surface modification of PTFE in this investigation. The impact strength of POM/AAc-*g*-PPTFE composites was more than twice of that of POM/PTFE composites. The Taber wear factor and friction coefficient of POM/AAc-*g*-PPTFE composites decreased markedly. © 2000 John Wiley & Sons, Inc. J Appl Polym Sci 78: 800–807, 2000

Key words: POM; PTFE; argon (Ar) plasma; AAc; Taber wear factor; friction coefficient

INTRODUCTION

Polyacetal (POM) resins are available as homopolymers and copolymers. They are plastics with strength approaching those of nonferrous metals. They are metal-like, strong, hard, highly crystalline thermoplastic with a unique balance of mechanical, thermal, chemical, and electrical properties.[1] Another characteristic of POM resin is their good wear resistance. Consequently, they are applied as the rotating materials of mechanical, electromechanical, and electronic parts. The inherent properties of POM including wear resistance and low coefficient of friction are imparted by additives such as PTFE,[2–6] carbon fiber,[7–10] oil,[11,12] aramide fiber,[13,14] or mixtures of several additives.[15–18] These additives make the resin an excellent material for functional parts including cams, gears, valve seat, stem parking, bearings, thrust washers, and seals. However, in some applications the wear resistance of POM still cannot meet the requirements. Further improvement in wear resistance of POM is necessary.

To increase wear resistance and decrease friction coefficient of POM, the authors added PTFE fiber as the filler in POM. The PTFE exhibits a very low coefficient of friction, and it can easily form a thin film on the contact surfaces in the polymer composites. Nevertheless, fluoropolymers such as PTFE, tetrafluoroethylene–hexafluoropropylene copolymer (FEP), or polychloro-

Correspondence to: C.-Y. Huang.

Contract grant sponsor: National Science Council; contract grant number: NSC-85-2216-E-036-005.

Journal of Applied Polymer Science, Vol. 78, 800–807 (2000)

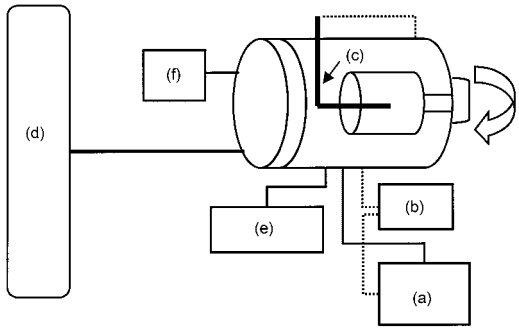

Figure 1 The self-designed rotary plasma reactor: (a) RF generator; (b) matching box; (c) electrode; (d) Ar gas; (e) vacuum pump; (f) vacuum gauge.

trifluoroethylene (PCTFE) usually have low wettability and bondability with other polymers. The adhesion between POM and PTFE is very weak. This makes the mechanical properties of POM/PTFE composites poor. In this study, the authors used Ar plasma treatment and graft techniques to modify the surface of PTFE fibers, so that the low surface energy of PTFE can be increased effectively. By such surface modification, the adhesion between PTFE fibers and POM could be increased, which leads to the improvement of friction, wear, and mechanical properties of POM/PTFE composites.

EXPERIMENTAL PROCEDURES

Materials

The PTFE fiber (L = 6 mm, L/D = 300) used in this study was a commercial product (Japan Showa Industry Co. Ltd.) designated as TOYOFLON 1200-180-200. The POM was a commercial product (Taiwan Engineering Plastics Co. Ltd.) designated as M90-02, with the following characteristics: specific gravity = 1.41 g/cm^3, melt flow index = 8–10 g/10 min. The acrylic acid (98%, Wako Chemical Ind.) was used after purification by distillation. Riboflavin($C_{17}H_{20}N_4O_6$, Sigma Chemical Co.) was used as purchased. An antioxidant, 2,2-Methylene bis-(4-methyl-6tert Butylphenol) (EP grade, made by Japan Tokyo Kasei), was also used as purchased.

Argon Plasma Treatment

A schematic diagram of the main part of the self-designed rotary glow discharge reactor used in this work is represented in Figure 1. The size of the outer cylindrical stainless steel vacuum chamber was about dia. = 30 cm, L = 20 cm. The size of the inner rotary mixing cylinder was about dia. = 15 cm, L = 15 cm, which was driven by a vacuum motor. The electrodes were in the form of columnar Cu stick stretching to the center of the inner cylinder. The PTFE fibers were put in the rotating inner cylinder and subjected to Ar plasma treatment. Prior to the start of plasma, the pressure in the chamber was reduced to 150 mTorr by a vacuum pump. Then the pure argon (99.999%) gas was introduced into the stainless steel chamber maintain a pressure at about 250 mTorr by adjusting the microthrottle valve on the Ar-inlet tube. After the pressure became stable, plasma was started by a RF power generator (13.56 MHz) operating at 20 watts. The plasma treatment time was 5–30 min.

UV-Induced AAc Graft Polymerization

After plasma treatment was done, the plasma pretreated PTFE fibers (PPTFE) were exposed to the laboratory atmosphere for about 5 min before grafting. In grafting polymerization with AAc (AAc-*g*-PPTFE), the PPTFE fibers were placed in an airtight, cylindrical bottle containing an aqueous solution of 400 mL of AAc and 100 mL of 0.02 g/L riboflavin. Then the bottle was put in between two UV light sources, which were halide lamps of 300 W. The distance from the UV light sources to the bottle was 10 cm. The exposure time was designed to be 5 min, 10 min, and 30 min. The concentrations of AAc solution for grafting were 5 wt % or 10 wt %, or 20 wt %.

FTIR Spectra

The characteristic absorption peaks of functional groups of PPTFE or AAc-*g*-PPTFE fibers were detected by a JASCO FT/IR-300E IR (infrared) spectrometer. For FTIR measurement, infrared spectra were obtained with spectrometer in polarized reflection (PR) method. The PR method makes good use of light parallel to the incident angle, thus removing the perpendicular elements of the incident light. It is, therefore, used for measurement of an extremely thin film (20 Å to 3 μm) on the polymer surface.

Blending

After plasma treatment and graft polymerization, the fibers were continuously blended with POM by melting (180°C) and rotary (30 rpm) mixing in

a Brabender Plasti-Corder Torque Reometer (PLE-330). During blending, POM and PPTFE or AAc-*g*-PPTFE were added into the Brabender with weight ratios of 100/0, 95/5, 90/10, 85/15, and 80/20 of POM/PPTFE. All the composites were added with 0.2 phr of antioxidant. Each blending of composite was completed in 10 min.

Friction Coefficient

The coefficient of friction was measured according to ASTM D1894-90 test method with a friction testing machine (model 1055D, Kayeness Inc.).

Taber Wear Factor

The Taber wear factor of each specimen was measured according to ASTM D1044 by a Taber wear machine (model 5130). Taber resistance measurements were run with HV-22 wheels under a load of 1 kg at ambient temperature (ca. 30°C). Taber wear factor was the loss mass in milligram per one thousand cycles of abrasion. The unit of Taber wear factor is mg/1000 cycles.

Mechanical Properties

Tensile properties were measured according to ASTM D638 using an Instron universal testing machine (model 4400). The samples were stretched with a 500 kg load cell at a drawing speed of 5 mm/min. Notched Izod-impact strength was measured according to ASTM D256, and impact energy was 60 kg-cm.

RESULTS AND DISCUSSION

FTIR Spectra

FTIR spectra of PTFE fibers after various treatment conditions were illustrated in Figure 2. When FTIR was operated in the PR method, incident and polarized angles were set constant at 80° and +90°, respectively. Under such a condition, measurement depth of samples was about 20 Å. The FTIR spectra of PTFE fibers after various plasma treatments and the spectrum of original PTFE fiber all showed that the rocking and wagging absorption of CF_2 appeared at 503 cm^{-1} and 620–640 cm^{-1}, respectively. In addition, a strong vibration absorption of CF_2 was observed at 1272 cm^{-1}. In his report, Wu[19] mentioned that a strong vibration absorption of CF_2 appeared at 1200–1350 cm^{-1}. On the PPTFE fiber (20 W, 30 min),

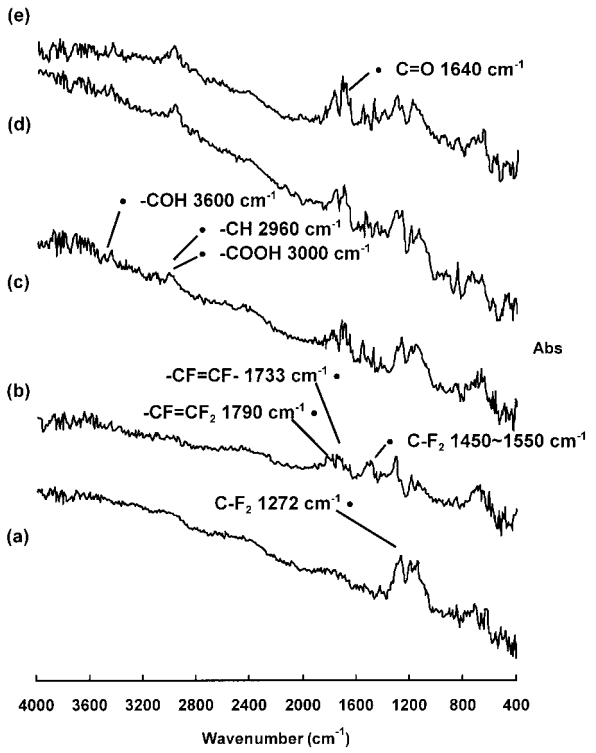

Figure 2 The FTIR spectra of various kinds of fibers: (a) PTFE; (b) PPTFE; (c) AAc (20 wt %)-g (5 min)-PPTFE (20 W, 30 min); (d) AAc (20 wt %)-g (10 min)-PPTFE (20 W, 30 min); (e) AAc (20 wt %)-g (30 min)-PPTFE (20 W, 30 min).

asymmetric stretching absorption of CF_2 appeared at 1450–1550 cm^{-1}. The absorption of —CF=CF— and —CF=CF_2 appeared at 1733 cm^{-1} and 1790 cm^{-1}, respectively. The —CF=CF— bond formation on the plasma-treated PTFE surface also had been shown by X.P.S.[20] These results suggested that fluorine atoms on the surface of PTFE fiber were impacted by high-energy ionization gas. Because of defluorination, the structures of surface molecule were changed as described above. Figure 2 shows that the intensities of CF_2 vibration absorption at 1272 cm^{-1} were decreased upon defluorization. Well[21] treated PTFE[21] with an Ar ion beam to modify its surface, and he reached the same conclusions. Huang and Chiang[22] also reported that the surface of the Na–naphthalene complex-treated PTFE powder formed the —CF=CF— double bond structure. In this investigation, the activators will be homogeneously introduced on the surface of the PTFE fiber by Ar plasma. Consequently, the plasma-treated PTFE fiber can be grafted with monomer acrylic acid (AAc) at these

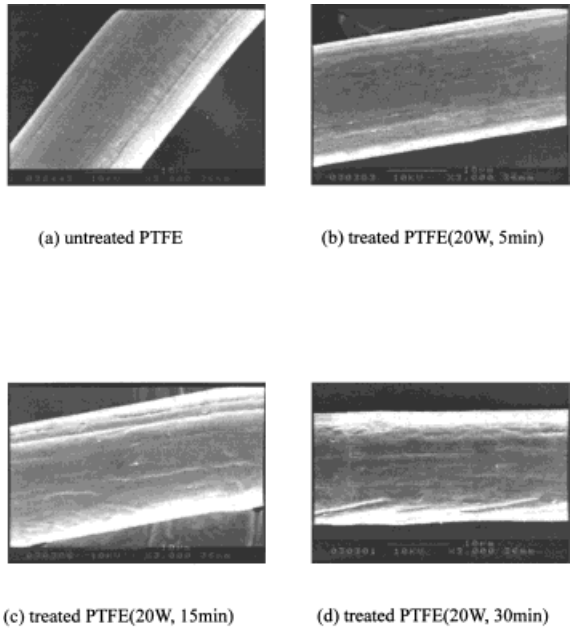

Figure 3 SEMs of the PPTFE fibers surface with various plasma-treated times.

active sites of the fibers under the irradiation of the UV light.

Functional groups of AAc were observed on FTIR spectra of AAc-*g*-PPTFE fibers. PPTFE fibers that were grafted in the 20 wt % AAc solution by UV light for 5, 10, and 30 min were illustrated in Figure2(c–e) curves, respectively. The formation of —OH (3600 cm^{-1}), —CH (2960 cm^{-1}), —COOH (3000 cm^{-1}), and C=O (1640 cm^{-1}) structures were observed on these spectra. In addition, the intensity of —COOH (3000 cm^{-1}) and C=O (1640 cm^{-1}) absorption peaks increased with increasing the UV grafting time. However, it was observed that the intensity of vibration absorption of CF_2 decreased with increasing UV grafting time. It was because that the thickness of AAc that grafted on the surface of AAc-*g*-PPTFE fiber increased with increasing UV grafting time. This phenomenon was also evident in SEM observations, and will be discussed in the next section. Yang and Chen[22] also succeeded in grafting acrylamide onto the surface of plasma-treated PTFE films.

SEM

It could be observed, from Figure 3, that the surface morphology of PTFE fiber changed with various treating time under 20 W plasma treatment. After 5 min treatment, the smooth surface of original PTFE fibers became rough [Fig. 3(b)]. The roughness of surface increased with increasing treatment time. These phenomena were caused by the defluorization after plasma treatment.

Figure 4 revealed the changes of surface morphology of AAc-*g*-PPTFE fiber that were treated by 20 W plasma for 30 min, followed by grafting under UV light for 5 min in AAc solutions of various concentrations. The SEM revealed that the surface of AAc-*g*-PPTFE fiber that was grafted in 5 wt % AAc solution was generally smooth. But silk-like fiber of AAc was also observed on some surface of AAc-*g*-PPTFE fibers. On the surface of AAc-*g*-PPTFE fibers that were grafted in 10 wt % AAc solution thin pieces of AAc could be observed. However, on the surface of AAc-*g*-PPTFE fibers that were grafted in 20 wt % AAc solution, island-like pieces of AAc were observed. The SEM micrographs showed that the thickness of grafted AAc increased with increasing the concentration of AAc in grafting solutions.

Mechanical Properties

Figure 5 reveals that the impact strength of POM was 5.23 kg-cm/cm. The impact strength was raised to 9.02 kg-cm/cm after 15 wt % PTFE fiber was added. Furthermore, the impact strength of POM/PPTFE was higher than that of POM/PTFE. This was because that after PTFE fiber was

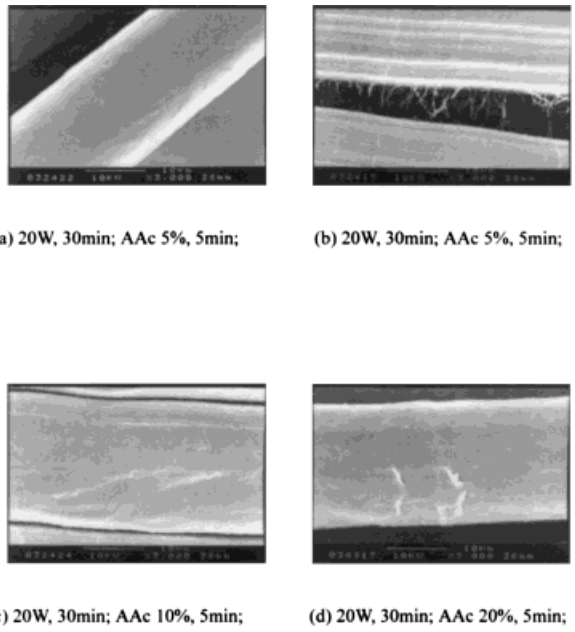

Figure 4 SEMs of the AAc-*g*-PPTFE fibers surface with various grafting concentrations of AAc.

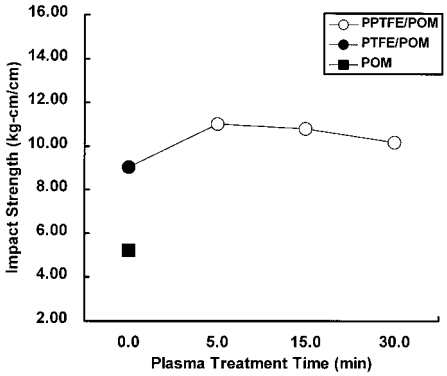

Figure 5 Impact strength vs. various plasma (20 W) treatment times of PPTFE fibers for POM/PPTFE (85/15) composites.

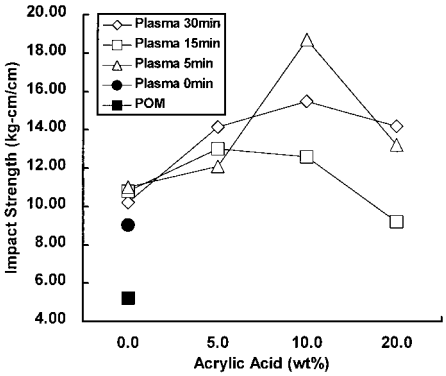

Figure 7 Impact strength vs. various AAc grafting concentrations of AAc-*g*(5 min)-PPTFE (20 W) fibers for POM/AAc-*g*(5 min)-PPTFE (20 W) (85/15) composites.

treated by plasma, surface energy increased and intermolecule bonding became better. Therefore, the compatibility between PPTFE fiber and POM became better. Figure 5 shows that the impact strength of POM/PPTFE composites tended to decrease with increasing the plasma treatment time. This was because that the longer the plasma treatment time, the more the free radicals, oxides, and peroxide contents on the surface of PPTFE fiber, which would break the backbones of POM. The same result was also revealed in tensile tests (Fig. 6). It could be learned from Figure 6 that the mechanical properties of POM/PPTFE composites were better than that of POM/PTFE composites in the respect of fracture strain and tensile strength. In addition, the fracture strain tended to increase with increasing the plasma treatment time. As far as physics was concerned, rough surface of PPTFE fiber offered a friction force; therefore, fracture strain increased.

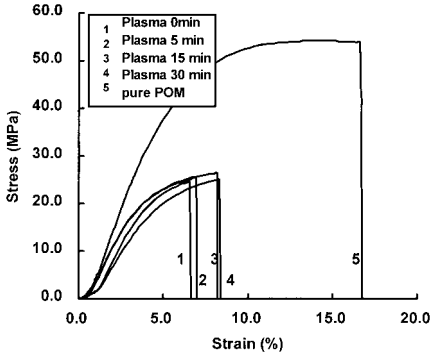

Figure 6 Stress–strain curves of POM/PPTFE (85/15) composites with various plasma (20 W) treatment time PPTFE fibers.

As far as the molecular structure was concerned, oxygen atom on the surface of the PPTFE fiber would attract the hydrogen atom in POM. Therefore, intermolecule bonding between POM and PPTFE fiber increased. On the other hand, free radicals and peroxides on the PPTFE fiber would destroy backbones of POM, leading to the decrease of tensile strength.

The SEM micrographs in Figure 4 showed that the thickness of grafted AAc on the AAc-*g*-PPTFE fiber surface increased with increasing the concentration of AAc. In addition, Figure 7 shows that the impact strength of POM/AAc-*g*-PPTFE composites significantly increased after AAc grafting onto the surface of PPTFE. Nevertheless, too much grafted AAc would lower the impact strength of composites. This was because when the thickness of grafting was too thick, attraction between AAc molecules was weak when compared with the attraction between AAc and PPTFE, or that between AAc and POM. Therefore, impact strength would decrease. To investigate the morphologies of the composites, the cryofractured surface of composites specimens were examined by scanning electron microscopy. Figure 8(a) shows that the PTFE fiber surface of the fractured POM/PTFE composite was still smooth (impact strength 9.02 kg-cm/cm). Separation at the interface between PTFE fiber and POM was very obvious. But separation at the interface between POM and PPTFE fiber in POM/PPTFE was not obvious [Fig. 8(b)]. This accounted for the fact that the impact strength of POM/PPTFE was greater than that of POM/PTFE. SEM micrographs of fractured POM/AAc (10 wt %)-g (5 min)-PPTFE composites (impact strength 18.71 kg-cm/cm) was shown in Figure 8(c). It clearly shows

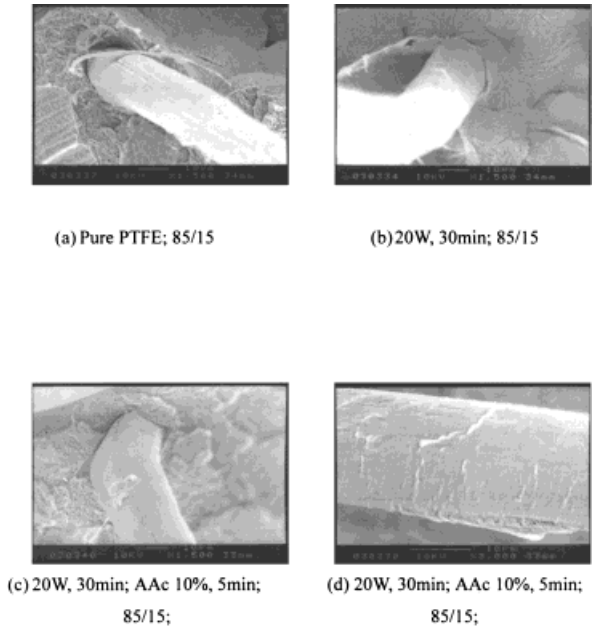

Figure 8 The SEM micrographs of fractured surface of various composites.

that POM attached on the surface of AAc-*g*-PPTFE fibers after fracture. Figure 8(d) was an enlarged view of the fiber in Figure 8(c). In addition to strip grafting of AAc on the AAc-*g*-PPTFE fiber, POM also adhered at the bottom-right of the fiber.

Figure 9 shows the stress–strain curves for PTFE fiber-reinforced POM. After surface modification of PTFE fiber, the tensile strength increased. Besides, the strain of POM/AAc-*g*-PPTFE was also greater than that of POM/PTFE. This was because the adhesion between the AAc-*g*-PPTFE fiber and POM was improved by grafting AAc onto the surface of the PPTFE fiber.

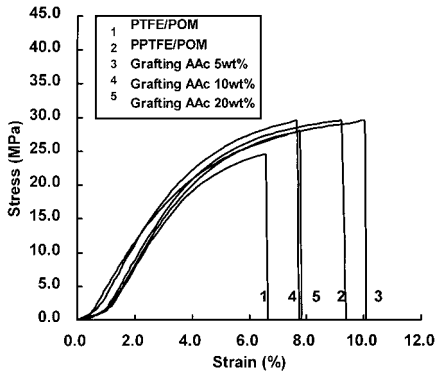

Figure 9 Stress–strain curves of POM/AAc-*g*(5 min)-PPTFE (20 W, 30 min) (85/15) composites with various AAc grafting concentrations.

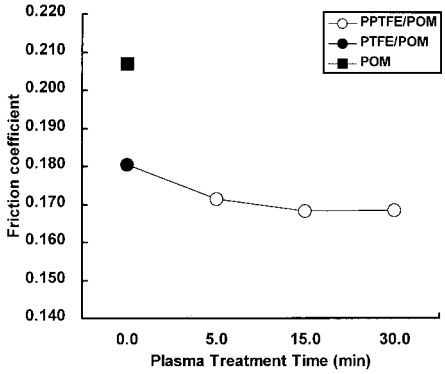

Figure 10 Friction coefficient of POM/PPTFE (85/15) composites with various plasma (20 W) treatment time PPTFE fibers.

Friction Coefficient

Decreasing friction coefficient was one of the most important purposes of this investigation. It could be observed from Figure 10 that friction coefficient of POM was 0.206, and it decreased to 0.180 after 15wt % PTFE fiber was added. In addition, it decreased to 0.16–0.17 after 15 wt % PPTFE fiber was added. The main reason that lead to the decreasing in friction coefficient of POM/PTFE composites was that lubricant PTFE fiber lowered the adhesion between frictional surface. Because surface energy of the PPTFE fiber was higher than that of the PTFE fiber, the PPTFE fiber had better compatibility with POM. Therefore, dispersion of the PPTFE fiber in POM was better than that of the PTFE fiber in POM. This could decrease the friction coefficient.

Figure 11 shows the friction coefficient of POM/AAc-*g*-PPTFE (85 wt %/15 wt %) under various grafting concentrations of AAc onto the surface of the PPTFE fiber. It could be seen from this figure that the friction coefficient of POM could be efficiently lowered after the PTFE fiber was added to POM. In addition, the PPTFE fiber would be evenly dispersed in POM, and the friction coefficient of PPTFE/POM composites was decreased. As the AAc-*g*-PPTFE fiber was added into POM, the friction coefficient of composites could be decreased further. It was suggested that the dispersion of the AAc-*g*-PPTFE fiber in POM could be improved by using grafted AAc onto the surface of PPTFE, thus decreasing the friction coefficient of polymers.

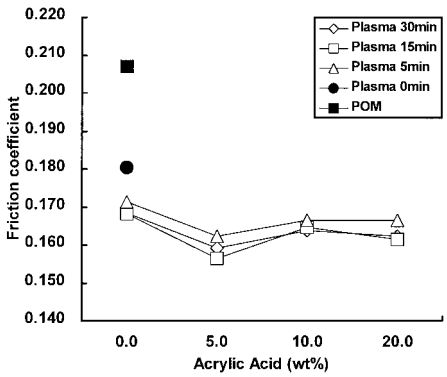

Figure 11 Friction coefficient of POM/AAc-*g*-PPTFE (20 W, 30 min) (85/15) composites with various AAc grafting concentrations.

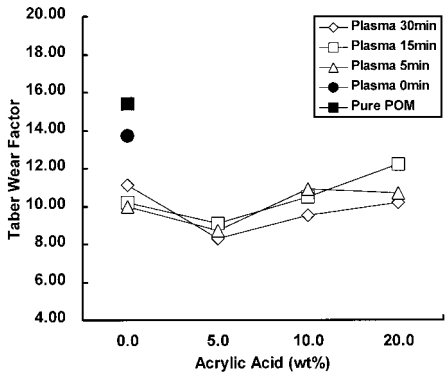

Figure 13 Taber wear factor of POM/AAc-*g*-PPTFE (20 W, 30 min) (85/15) composites with arious AAc grafting concentrations.

Taber Wear Factor

It could be observed from Figure 12 that Taber wear factor of POM was 15.4, and it decreased to 14.7 after 15 wt % PTFE fiber was added. It became even lower after 15 wt % PPTFE was added. This was because the PPTFE fiber had better dispersion. However, Figure 12 shows that the Taber wear factor of PPTFE/POM increased with increasing the plasma treatment time. Two reasons lead to this phenomenon: first, after a long treatment time of the plasma, the surface of PTFE was easy to fissure and uncover. Therefore, the Taber wear factor increased. Second, more free radicals and peroxides would appear on the PPTFE fiber that was treated by plasma for a long time. The split of POM happened when blending, leading to the increase of Taber wear factor.

Figure 13 clearly shows that the Taber wear factor of composites increased with increasing the AAc concentration of grafting. After PPTFE fiber was grafted in AAc solution, the AAc-*g*-PPTFE fiber dispersion in the POM became better, and the Taber wear factor lowered. But when the AAc concentration of grafting became high, AAc that was grafted on the surface of the fiber became the main reason that led to the increase of the Taber wear factor. When wheels rolled over composites, the first material that wheels touched was the AAc film on the AAc-*g*-PPTFE fiber instead of PTFE. When AAc interacted with wheels, it would not transform to the worn surface and form lubricant film as PTFE would. Instead, some small grains were formed, and stayed on the worn surface. These small grains would form tracks on the POM with wheels, thereby leading to the increase of the Taber wear factor. When quantities of grafting increased, more small grains of AAc would form, thereby producing more wear.

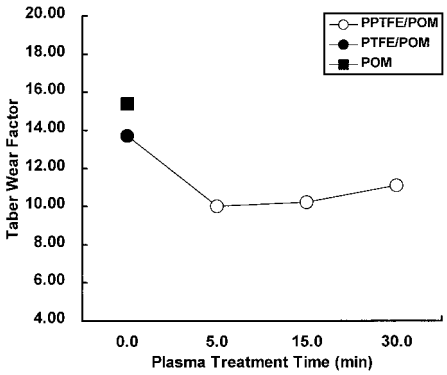

Figure 12 Taber wear factor of POM/PPTFE (85/15) composites with various plasma (20 W) treatment time PPTFE fibers.

SEM was used to examine the composites that possessed the highest and the lowest value of Taber wear factor. Figure 14(a) shows the worn surface of POM. As for Figure 14(b), this shows the worn surface of the POM/PTFE composites. It could be observed from Figure 14(b) that PTFE transformed to the worn surface of composites and one layer of lubricant film was formed. Figure 14(c) was the worn surface of POM/AAc (5 wt %)-g (5 min)-PPTFE(20 W, 30 min) (Taber wear factor 8.3). Figure 14(c) shows that a layer of lubricant film distributed evenly on the worn surface; therefore, it could be inferred that this composite possessed good wear resistant property. Figure14(d) shows the worn surface of POM/AAc (20 wt %)-g (5 min)-PPTFE (20 W, 15 min) (Taber wear factor 11.9). In Figure 14(d), no lubricant

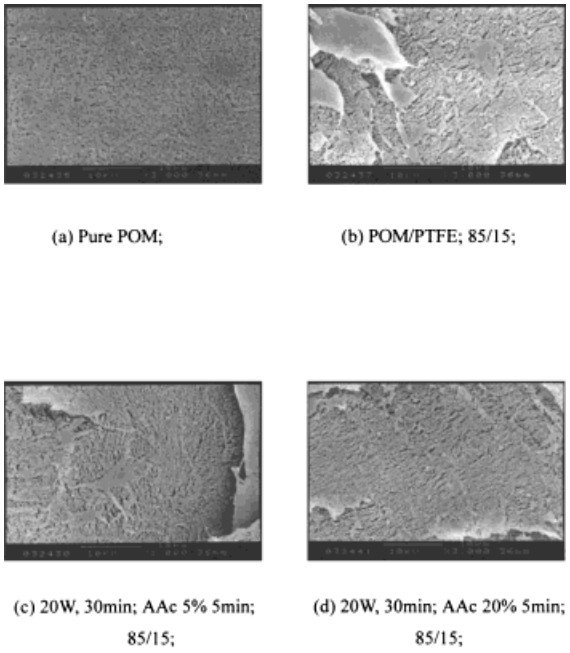

Figure 14 The SEM micrographs of worn surface of various composites.

film could be seen on the worn surface, but many white grains appeared. These grains were AAc scraps, which were the main reason leading to the increase of the Taber wear factor.

CONCLUSIONS

Cylinder plasma equipment can be used to modify PTFE fiber efficiently. When the plasma-treated fiber is tested by PR-FTIR, C=C, and oxygen content would be observed. The longer the treating time of plasma, the lower the impact strength of POM/PPTFE composites.

Friction coefficient and Taber wear factor of the POM/PTFE composites were lowered after the PTFE fiber was treated by plasma. In addition, the dispersion of PTFE fiber in POM is improved after PTFE fibers were treated by plasma. From IR measurement of AAc-*g*-PPTFE fiber, the structures of C=O, COOH, and COH were revealed on the surface of the AAc-*g*-PPTFE fiber. Both SEM photographs and mechanical testing curves show that lower grafting quantities of AAc onto fiber resulted in stronger bonding between the fiber and matrix. High grafting quantities would decrease the mechanical strength and strain. High grafting quantities would also increase friction coefficients of composites, thereby increasing the Taber wear factor. Because AAc is not a substance with low friction coefficient, when they cover PTFE fiber with huge amounts, lubricant characteristics of PTFE would not show up.

The authors express their sincere appreciation to Dr. T. S. Lin, President of Tatung University, for his encouragement and support. Thanks are due to the National Science Council for Financial support under contract number NSC-85-2216-E-036-005.

REFERENCES

1. Plastic Engineering, Engineering Resins Primer, 1974, December, 30, 20.
2. Chiang, W. Y.; Huang, C. Y. J Chin I 1991, 22, 291.
3. Chiang, W. Y.; Huang, C. Y. Angew Makromol Chem 1992, 196, 21.
4. Chiang, W. Y.; Huang, C. Y. Eur Polym J 1992, 28, 583.
5. Chiang, W. Y.; Huang, C. Y. J Appl Polym Sci 1993, 47, 577.
6. Huang, C. Y.; Chiang, W. Y. Eur Polym J 1993, 29, 843.
7. Chiang, W. Y.; Huang, C. Y. Compos Polym 1991, 4, 251.
8. Brown, S. A. Polym Mater Sci Eng 1985, 53, 494.
9. Jain, V. K. Wear 1983, 92, 279.
10. Jain, V. K. Wear Mater 1983, 583.
11. Takahashi, H.; Iwata, K. Jpn Kokai Tokkyo Koho, JP 63, 179, 958.
12. Matsuo, T.; Mori, S.; Yokota, N. Jpn Kokai Tokkyo Koho, JP 61, 12, 743.
13. Waston, K. R.; Wu, Y. T.; Riewald, P. G. Plast Eng 1989, 45, 83.
14. Parlow, G. Gummi, Fasern, Kunstst 1988, 41, 608.
15. Kitamura, A.; Kawamura, M. Jpn. Kokai Tokkyo Koho, JP 61, 76, 594.
16. Bando Chem. Industries, Ltd., Jpn. Kokai Tokkyo Koho, JP 59, 179, 653.
17. Suzuki, K.; Ogahama, M. Jpn. Kokai Tokkyo Koho, JP 62, 04, 748.
18. Jinno, O.; Fukuoka, T. Jpn. Kokai Tokkyo Koho, JP 62, 10, 165.
19. Wu, S. In Polymer Interface and Adhesion; Marcel Dekker, Inc.: New York, 1982, p. 280.
20. Schonhorn, H.; Hansen, R. H. J Appl Polym Sci 1967, 11, 1461.
21. Wells, R. K.; Ryan, M. E.; Badyal, J. P. S. J Phys Chem 1993, 97, 12879.
22. Huang, C. Y.; Chiang, W. Y. Angew Makromol Chem 1993, 209, 9.
23. Yang, M. R.; Chen, K. S. Mater Chem Phys 1997, 50, 11.